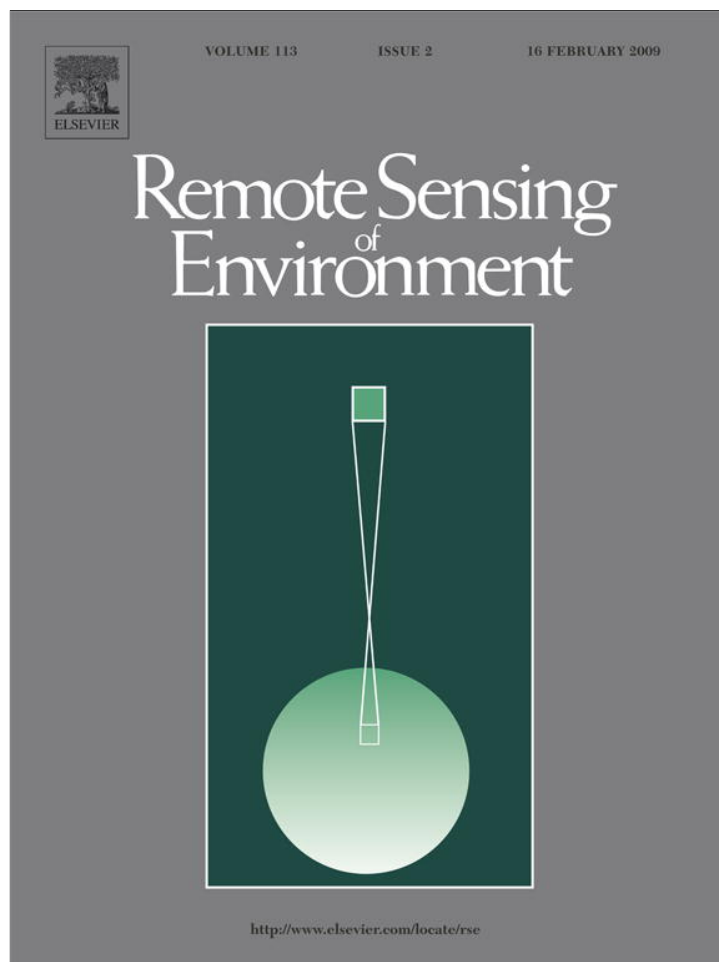


Provided for non-commercial research and education use.
Not for reproduction, distribution or commercial use.



This article appeared in a journal published by Elsevier. The attached copy is furnished to the author for internal non-commercial research and education use, including for instruction at the authors institution and sharing with colleagues.

Other uses, including reproduction and distribution, or selling or licensing copies, or posting to personal, institutional or third party websites are prohibited.

In most cases authors are permitted to post their version of the article (e.g. in Word or Tex form) to their personal website or institutional repository. Authors requiring further information regarding Elsevier's archiving and manuscript policies are encouraged to visit:

<http://www.elsevier.com/copyright>



Contents lists available at ScienceDirect

Remote Sensing of Environment

journal homepage: www.elsevier.com/locate/rse

Evaluation of the SMOS L-MEB passive microwave soil moisture retrieval algorithm

Rocco Panciera^{a,*}, Jeffrey P. Walker^a, Jetse D. Kalma^b, Edward J. Kim^c,
Kauzar Saleh^d, Jean-Pierre Wigneron^e^a Dept. of Civil and Environmental Engineering, The University of Melbourne, Australia^b School of Engineering, The University of Newcastle, Australia^c NASA Goddard Space Flight Center, USA^d Department of Geography, University of Cambridge, United Kingdom^e INRA, EPHYSE, Bordeaux, France

ARTICLE INFO

Article history:

Received 26 July 2008

Received in revised form 14 October 2008

Accepted 18 October 2008

Keywords:

Soil moisture

Microwave radiometry

SMOS

NAFE

ABSTRACT

Soil moisture will be mapped globally by the European Soil Moisture and Ocean Salinity (SMOS) mission to be launched in 2009. The expected soil moisture accuracy will be 4.0 %v/v. The core component of the SMOS soil moisture retrieval algorithm is the L-band Microwave Emission of the Biosphere (L-MEB) model which simulates the microwave emission at L-band from the soil–vegetation layer. The model parameters have been calibrated with data acquired by tower mounted radiometer studies in Europe and the United States, with a typical footprint size of approximately 10 m. In this study, aircraft L-band data acquired during the National Airborne Field Experiment (NAFE) intensive campaign held in South-eastern Australia in 2005 are used to perform the first evaluation of the L-MEB model and its proposed parameterization when applied to coarser footprints (62.5 m). The model could be evaluated across large areas including a wide range of land surface conditions, typical of the Australian environment. Soil moisture was retrieved from the aircraft brightness temperatures using L-MEB and ground measured ancillary data (soil temperature, soil texture, vegetation water content and surface roughness) and subsequently evaluated against ground measurements of soil moisture. The retrieval accuracy when using the L-MEB ‘default’ set of model parameters was found to be better than 4.0 %v/v only over grassland covered sites. Over crops the model was found to underestimate soil moisture by up to 32 %v/v. After site specific calibration of the vegetation and roughness parameters, the retrieval accuracy was found to be equal or better than 4.8 %v/v for crops and grasslands at 62.5-m resolution. It is suggested that the proposed value of roughness parameter H_R for crops is too low, and that variability of H_R with soil moisture must be taken into consideration to obtain accurate retrievals at these scales. The analysis presented here is a crucial step towards validating the application of L-MEB for soil moisture retrieval from satellite observations in an operational context.

© 2008 Elsevier Inc. All rights reserved.

1. Introduction

Near-surface soil moisture retrieval from L-band (1.4 GHz) passive microwave brightness temperature (TB) measurements has been demonstrated from tower (Jackson et al., 1982; Wang, 1983) and airborne experiments (Jackson et al., 1984; Njoku et al., 2002). Current passive microwave algorithms for soil moisture retrieval are based on inversion of radiative transfer models which simulate the microwave emission from the earth surface given knowledge of the vegetation cover type and water content, surface soil temperature, surface roughness, and soil texture (Jackson, 1993; Wigneron et al., 1995). These models assume homogeneous conditions within each pixel, and have been developed from radiometer observations of homogenous

pixels in Europe and the United States with resolutions on the order of 10's of meters.

The first satellite to make L-band observations specific to soil moisture retrieval will be the European Soil Moisture and Ocean Salinity (SMOS) mission (Kerr et al., 2001), to be launched in 2009. The baseline SMOS payload is an L-band (1.4 GHz) two dimensional (2D) interferometric radiometer that aims at providing global maps of soil moisture with an accuracy better than 4 %v/v every 3 days and with a resolution better than 50 km (Kerr et al., 2001). SMOS operations will make use of the so called ‘SMOS L2’ processor to retrieve soil moisture and other surface parameters (e.g. vegetation optical thickness and roughness) taking advantage of the dual-polarised multi angular TB observations this sensor will provide. The core of the SMOS L2 processor is the inversion of the L-band Microwave Emission of the Biosphere (L-MEB) model (Wigneron et al., 2007), which is used as a forward emission model to simulate the L-band emission of the soil–canopy layer at Vertical and Horizontal polarisation (V-pol, H-pol) according to incidence angle. The L-MEB model was developed from an

* Corresponding author. Department of Civil and Environmental Engineering, The University of Melbourne, Parkville, Victoria 3010, Australia. Tel.: +61 3 8344 4955; fax: +61 3 8344 6215.

E-mail address: rocco@civenv.unimelb.edu.au (R. Panciera).

extensive review of the current knowledge of the microwave emission of various land cover types (Wigneron et al., 2003) and has been tested with tower based studies on mostly homogeneous land surface conditions of low to moderate vegetation density, such as crops and grass-type surfaces (Wigneron et al., 2001; De Rosnay et al., 2006; Saleh et al., 2006b, 2007; Escorihuela et al., 2007). Development is also ongoing for forested, rough terrain and frozen surfaces (Della Vecchia et al., 2007; Grant et al., 2007; Talone et al., 2007). In order to retrieve soil moisture from SMOS data, the algorithm requires information on the vegetation and surface type dependent parameters of the emission model, such as the vegetation opacity, vegetation scattering albedo and roughness. A summary of published parameters for a variety of land cover types has been recently completed (Wigneron et al., 2008) and will be hereby referred to as the L-MEB 'default' parameter set.

To date the L-MEB model and its proposed parameterization has not been widely tested. There is therefore a strong need for an evaluation of the L-MEB model across a diverse range of land surface conditions globally. Consequently, this study rigorously evaluates the L-MEB model under Australian conditions for grassland and crop land cover types, using L-band aircraft data from the National Airborne Field Experiment conducted in south-eastern Australia in 2005 (NAFE'05).

2. Data

The NAFE'05 experiment was conducted in the Goulburn river catchment, in South-eastern Australia, with the aim to provide passive microwave airborne data supported by ground measurements of soil moisture for algorithm development and downscaling studies. A complete description of the experiment is provided in Panciera et al. (2008) so only the pertinent details are provided here. The general climate within the region can be described as subhumid, with average annual rainfall of 700 mm (maximum in October/November of about 50 mm), average annual pan evaporation of 1800 mm and monthly mean maximum temperatures varying between 30 °C in summer and 14 °C in winter, with minimum values of 16 °C and 2 °C, respectively. The catchment has an extensive network of *in situ* surface and meteorological observations and has been the location of several remote sensing related experiments (Rüdiger et al., 2007; Panciera et al., 2008). The data acquisition phase of NAFE'05 took place between October 31st and November 25th, 2005, and included passive microwave and thermal infrared airborne observations at multiple resolutions. The land cover

conditions in the Goulburn catchment during the field experiment included grasslands, crops (wheat, barley, sorghum and oats), open woodland and forest, with the last two mainly concentrated in the southern part of the study area (see Fig. 1). Soil properties in the area are highly variable, including clay soil in the northern part and sandy soil in the southern part of the study area. The topography in the area is gentle with some flat alluvial areas around the main streams.

TB data were acquired daily at multiple resolutions over two focus areas: the Krui area of approximately 10 km×30 km (western part of the study area; see Fig. 1) and the Merriwa area of approximately 15 km×30 km (eastern part). Each area was mapped entirely at various resolutions on alternate days, with flights beginning at around 6:00AM and ending by 2:00PM. The observations used in this study (62.5 m resolution) were acquired between approximately 9:00AM and 11:00AM. Parallel South–North oriented flight-lines were flown to cover the area with a 1/6th of the swath (i.e., one beam) overlap. Favorable meteorological conditions during the experiment allowed the observation of several wetting and drying cycles. At the beginning of the experiment heavy rainstorms crossed the study area, delivering approximately 10 mm of cumulative rainfall, followed by more intense rainfall on November 5th, 10th and 23rd (approximately 20 mm in the eastern part of the catchment and 10 mm in the western part).

2.1. High resolution ground monitoring sites

Soil moisture was retrieved at eight locations corresponding to high resolution ground sampling sites (Fig. 1), which were intensively ground monitored for top 5 cm soil moisture, soil temperature, surface roughness, soil texture, vegetation biomass and vegetation water content. The location and extent of these sites were carefully chosen with the objective of characterizing the variety of land covers, soil type and topography present in the study area. Details of the high resolution sites land cover, surface and soil type conditions are summarized in Table 1. The Roscommon site was considered a 'control' site as it exhibited uniform, flat, short grass conditions. All other sites were characterized by either heterogeneous land cover (Midlothian, Cullingral, Illogan and Pembroke) or significant topography (Stanley and Dales and Merriwa Park). A total of 4 concurrent air- and ground-borne mappings were available for each high resolution site across the 4 week long campaign.

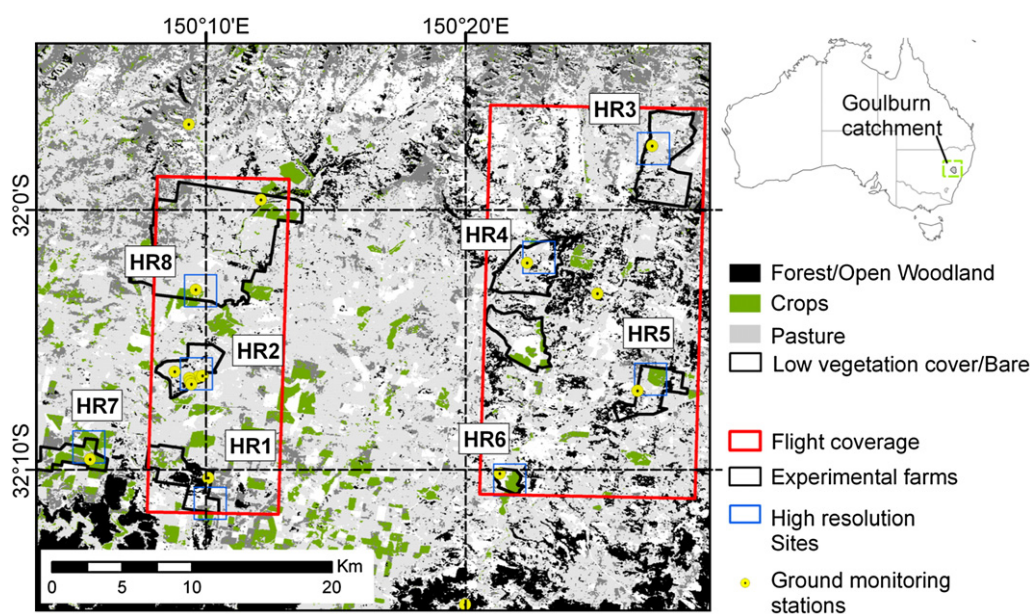


Fig. 1. The NAFE'05 study area layout, airborne and ground sampling areas extent and permanent monitoring stations. The ground sampling high resolution sites are labelled with HR1–8.

Table 1
Characteristics of the high resolution ground sampling sites

Fig. 1 code	High resolution site	Land cover	Topography	Vegetation water content [kg/m ²] max–min	% sand	% clay	Standard deviation of roughness heights [mm] mean (stdev)	Correlation length of roughness [mm] mean (stdev)
HR1	Roscommon	Grassland	Flat	1.1–0.4	67 ^a	15 ^a	6.3 (1.0)	64.7 (36.8)
HR2	Stanley	Grassland	Sloping	0.4–0.1	6	54	10.8 (3.7)	93.9 (45.1)
HR3	Dales	Grassland	Sloping	0.8–0.2	31	51	9.1 (2.3)	65.4 (37.6)
HR4	Midlothian	Fallow/Lucerne	Flat	0.3–0.1	10	69	8.3 (3.6)	83.9 (38.1)
HR5	Merriwa Park	Wheat	Gently sloping	2.0–1.2	21	36	7.5 (2.7)	93.4 (54.2)
HR6	Cullingral	Wheat/Barley	Flat	0.9–0.4	30 ^a	26 ^a	6.6 (2.4)	104.8 (53.4)
HR7	Illogan	Oats/Barley	Across Gully	1.1–0.3	26	23	9.8 (3.6)	61.7 (43.5)
HR8	Pembroke	Wheat/Barley	Gently sloping	2.4–2.0	6	71	8.5 (2.8)	98.0 (53.6)

^a Indicate soil texture data estimated from 5 cm soil samples.

Spatial distribution of the top 5 cm soil moisture was monitored at each site once a week concurrently with airborne observations. An inherent difficulty in relating the soil moisture information derived by remote sensors to that of ground sampling devices used for validation is related to the fact that the two systems have different “supports” (i.e., the integration volume or area from where the signal is detected) which is of the order of cm's for soil moisture probes such and on the order of 100's m for the airborne acquisitions. In this study this problem was addressed by performing ground sampling at very fine scale in order to characterise the spatial variation of soil moisture within the radiometer footprint. A 150 m×150 m core area was therefore sampled on a very fine regular grid (6.25 m and 12.5 m spacing) by a team of two people to provide detailed ground truthing of the high resolution footprints, while the surrounding areas were sampled at decreasing resolution (62.5 m to 500 m) in order to cover as large an area as possible (Fig. 2). This extensive sampling was achieved with the Stevens Water Hydraprobe dielectric soil moisture probes interfaced with a handheld PC, GPS positioning and GIS. The probes were calibrated with over 120 gravimetric field samples and subsequently in the laboratory, yielding an estimated accuracy of ±3.5 %v/v (Merlin et al., 2007). Soil moisture ground sampling took approximately 6–8 h daily (8:00AM–2:00PM), and flights over the sites were timed so that they always fell within this time window (9:00AM–11:00AM). Surface soil moisture can vary significantly on a diurnal basis, especially for short vegetation. Daily changes in soil moisture during the ground sampling time window were therefore monitored at the eleven monitoring stations across the study area (all on native grass). Soil moisture was found to be stable between 8:00AM and 2:00PM, with a mean soil moisture decrease across all stations and all sampling days of less than 1.1 %v/v. Given that the airborne acquisitions were generally within the time window where this variation occurred, the differences between soil moisture

at the time of aircraft overpass and that of the ground monitoring will be even smaller than that indicated above.

Vegetation biomass and vegetation water content (VWC) were monitored throughout the campaign using 50 cm×50 cm biomass samples collected at the end of each sampling day at two fixed locations chosen to be representative of the site vegetation conditions. The VWC ranged from a minimum of 0.1 kg/m² for the short lucerne at Midlothian to a maximum of 2.4 kg/m² for the mature wheat crop at Pembroke, with an average of 0.4 kg/m² for grassland sites and 2 kg/m² for crop sites. As shown in Table 1, the VWC varied significantly throughout the campaign; as much as 1 kg/m² for crops. On two occasions during the campaign, the first and the last weeks, the spatial variability of the VWC across all high resolution sites was also characterized with 16 biomass samples (see Fig. 2). The spatial variability was generally small for all the grassland sites (standard deviation of 0.15 kg/m²) and most crop sites (0.4 kg/m²), but was significant in the case of the Pembroke site (1 kg/m²). The VWC is also known to have diurnal variation, mainly associated with the presence of dew on the plants in the early hours of the morning. To ensure that this wouldn't interfere with the aircraft microwave observations, leaf wetness sensors were installed at each high resolution site to continuously record the presence of dew. These data (confirmed also by field observation) indicated that at all eight high resolution sites dew had completely dried off by 8:00AM throughout the campaign. Therefore the VWC samples taken at the end of each sampling day were considered representative of the conditions observed at the time of aircraft overpasses.

A footprint-average value of soil temperature for each TB observation was estimated from the time-series of soil temperature recorded every 20 min at 2.5 cm depth at the nearby monitoring stations, making use of the L-band radiometer time for reference. Soil texture was determined by hydrometer analysis of 30 cm deep soil samples collected at or near the high resolution site. Despite the availability of soil texture data for similar 5 cm deep samples, the laser mastersizer particle size analysis performed on these samples is reported to consistently underestimate clay content, while it properly estimate the coarse fraction (Campbell, 2003), and therefore the 30 cm samples were preferred. The 5 cm sample was used in two cases only (Roscommon and Cullingral), as the 30 cm samples were clearly too far from the high resolution sites to be representative. As these sites are located in the southern part of the study area, which is dominated by sandstone derived soils (sandy), the laser particle analysis is expected to be sufficiently accurate in these cases. Finally, surface roughness parameters were estimated by taking 1 m-long transects of surface heights in two perpendicular directions in order to take into account anisotropy in surface roughness (common in ploughed cropped fields). Surface roughness heights and correlation lengths were very uniform across the eight sites, with an average of 8.4 mm and 83 mm respectively (see Table 1). Soil types covered the whole range observed in the study area, from very sandy at Roscommon to fine black clay at Pembroke.

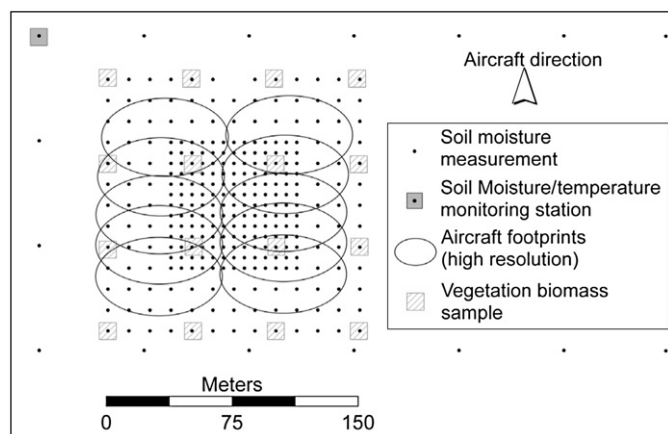


Fig. 2. Schematic of aircraft footprints and ground measurements at the high resolution ground sampling sites.

2.2. Airborne passive microwave radiometer observations

The passive microwave instrument used was the Polarimetric L-band Multibeam Radiometer (PLMR). The PLMR measured both V-pol and H-pol TB through 6 ellipses of 17° along-track and 13°–16.5° across-track with across track incidence angles of +/-7°, +/-21.5° and +/-38.5°. The PLMR was calibrated daily against ground targets (blackbody and clear sky) and the calibration further checked in-flight with overpasses of a nearby water body that was monitored for soil temperature and salinity. Complete details about the calibration procedures have been given by Panciera et al. (2008). The accuracy was estimated to be better than 0.7 K at H-pol and 2 K for V-pol; it is considered that on a bare smooth soil this corresponds to better than 1.0 %v/v soil moisture accuracy. The calibrated radiometer observations were geolocated taking into consideration the aircraft position, pitch, roll, and yaw information recorded for each measurement, with the beam centers projected onto a 250 m digital elevation model of the study area. The effective footprint size and ground incidence angle were also calculated taking into consideration the aircraft attitude, the terrain slope and beam geometry. Final processing included filtering data corresponding to elevated aircraft roll angles (higher than 10° from horizontal) corresponding to aircraft steep turns. This also minimises sun glint effect in the external beams.

3. The L-MEB model

The L-band Microwave Emission of the Biosphere model, L-MEB, is the core of the SMOS mission retrieval algorithm ('SMOS L2') and is based on a widely recognized approach to land emission simulation that uses a simplified (zero-order) radiative transfer equation (Wigneron et al., 1995; Jackson and Le Vine, 1996; Njoku et al., 2002). This model represents the soil as a flat surface in contact with the atmosphere, and the vegetation as a homogeneous layer. The soil emission is controlled by the microwave reflectivity of soil, which depends on the dielectric properties of the soil–water mixture, while the vegetation layer scatters and absorbs part of this radiation as well as emitting radiation itself. A complete description of the model has been given by Wigneron et al. (2007) so only a brief overview of the main model components is given here. The effects of soil and vegetation on the surface brightness temperature are represented in L-MEB by the so called 'τ-ω model' (Mo et al., 1982):

$$TB(\vartheta, P) = (1 - \omega_{\vartheta, P}) \left(1 - \gamma_{\vartheta, P} \right) \left(1 + \Gamma_{\vartheta, P} \gamma_{\vartheta, P} \right) T_V + (1 - \Gamma_{\vartheta, P}) \gamma_{\vartheta, P} T_{EFF} \quad (1)$$

where T_{EFF} and T_V are the effective soil and vegetation temperatures, ω and γ are respectively the single scattering albedo and the transmissivity of the vegetation layer, which vary in general with the measured polarisation P (horizontal or vertical) and the sensor observation angle ϑ . The reflectivity of a rough soil, Γ , that is also sensitive to the observation angle and measured polarisation, is controlled by the soil roughness parameters H_R and N_{RP} (Wang and Choudhury, 1981; Wigneron et al., 2001) by:

$$\Gamma = \Gamma^* \exp \left[-H_R \cos(\vartheta)^{N_{RP}} \right] \quad (2)$$

The reflectivity Γ^* of a smooth soil can be related to the surface soil moisture content through the Fresnel equations and a dielectric model, such as the Dobson dielectric mixing model currently used by L-MEB (Dobson et al., 1985), which takes into account soil textural properties to simulate the dielectric behavior of the soil–water mixture. Given that the Dobson model is well known to poorly represent very dry sandy soils, L-MEB switches to the Matzler dielectric model (Matzler, 1998) when soil moisture content is below 2 %v/v and sand fraction is above 90%.

The vegetation parameters in Eq. (1) are the single scattering albedo ω and the vegetation transmissivity γ . The latter is determined

by the vegetation optical depth at nadir, τ_{NAD} , and the parameters tt_V and tt_H (or tt_H and the parameter $R_{tt} = tt_V / tt_H$) that correct the optical depth for non-nadir views at each polarisation by:

$$\gamma(\vartheta, P) = \exp \left[-\tau_{NAD} \left(\cos^2(\vartheta) + tt_P * \sin^2(\vartheta) \right) \cos^{-1}(\vartheta) \right] \quad (3)$$

The optical depth at nadir τ_{NAD} increases with increased water in/on the vegetation, and consequently reduces the transmission of the soil brightness temperature across the vegetation, and can be related linearly to the VWC (kg/m²) using the so-called "b" parameter through $\tau_{NAD} = b * VWC$ (Jackson and Schmugge, 1991; Van de Griend and Wigneron, 2004). The canopy optical depth has been shown to increase significantly in response to rainfall, due to the dielectric properties of water intercepted by plants (Saleh et al., 2006a). In the SMOS L2 retrieval algorithm the effect of rainfall is not modeled, and data will be flagged for interception depending on a polarisation index. This study follows the same approach, with days immediately following significant rainfall events excluded from the analysis.

The soil effective temperature T_{EFF} should be calculated taking into account the soil temperature profile in the entire soil column which contributes to the emission (2 to 5 cm at L-Band). In L-MEB a novel formulation is used that calculates T_{EFF} as a function of two temperature measurements, one at the soil surface (T_{SURF}) and the other at a greater depth (T_{DEPTH}) (Wigneron et al., 2001) by:

$$T_{EFF} = T_{DEPTH} + (T_{SURF} - T_{DEPTH}) * (\theta / w_0)^{b_0} \quad (4)$$

Here θ stands for the top 5 cm soil moisture. Parameters w_0 and b_0 were calibrated using data from the SMOSREX experiment (De Rosnay et al., 2006), using soil temperatures at 2 cm and 50 cm respectively for T_{SURF} and T_{DEPTH} . Due to the lack of soil temperature measurements deeper than 15 cm at all the soil moisture monitoring stations in this study Eq. (4) was applied assuming that the value of soil temperature at 15 cm depth is a good estimate of T_{DEPTH} . This assumption was verified with soil temperature data at 15 cm and 60 cm collected at a meteorological stations located at the Stanley farm. The 60 cm temperature was found to have a positive bias of 0.9 K with respect to that at 15 cm, with an error standard deviation of 1.1 K. This impacts the calculation of T_{EFF} only on very dry conditions (when the effect T_{DEPTH} is important), yielding an error of less than 0.6 K, which is not significant for soil moisture retrieval purposes.

3.1. Optimisation scheme

In this study the forward emission model (2) is inverted to solve two different optimisation problems: (i) the retrieval of soil moisture given *a priori* (prescribed or calibrated) values for the vegetation and soil surface dependant parameters given TB; and (ii) the calibration of model vegetation and soil surface parameters given ground measured soil moisture and TB. The number of parameters that can be retrieved simultaneously depends on the number of simultaneous and independent TB's available under different measurement configurations (i.e., polarisation and incidence angle). In this study both soil moisture retrieval and calibration problems were solved through iterative least squares minimisation of the cost function:

$$CF = \frac{\sum \left(TB_{\vartheta, pol}^o - TB_{\vartheta, pol} \right)^2}{\sigma_{TB}^2} + \frac{\sum \left(p_i - p_i^{ini} \right)^2}{\sigma_p^2} \quad (5)$$

The cost function in Eq. (5) includes the classical cumulative squared error between simulated and measured brightness temperatures (TB and TB^o respectively), and an additional term which accounts for the squared error between the current value (p_i) and the initial guess (p_i^{ini}) of each retrieved quantity (e.g. soil moisture in the soil moisture retrieval problem or parameters H_R , b , etc. in the calibration

problem). The second term in Eq. (5) allows the user to constrain the retrieved values about a physically plausible estimate for each parameter (p_i^{ini}) through the standard deviation associated with this estimate (σ_p). This optimisation method has been developed for the retrieval of surface parameters from SMOS data, where the possibility of constraining parameters values stems from the availability of the values retrieved on previous overpasses (Wigneron et al., 2007). However, in this study the constraints were not used (i.e. no *a priori* knowledge was assumed), in order to find the 'real' optimum for each quantity. Therefore the value $\sigma_p^2 = 1$ was used in all cases.

3.2. L-MEB default parameters

A considerable amount of research has been devoted in the past decade toward estimating a set of generic parameters for the ' τ - ω model' including a variety of vegetation and surface types. Building upon these studies, a set of parameters has been recently compiled by Wigneron et al. (2008). This parameter set is briefly reviewed here before being applied to the soil moisture retrieval.

The main component of the ' τ - ω model' is the vegetation optical thickness, whose attenuation properties can be related to the VWC using the so-called b parameter, which is in general dependent on the sensor frequency, polarisation and view angle, as well as on the vegetation structure (Jackson and Schmugge, 1991; Van de Griend and Wigneron, 2004). At L-band a value of $b = 0.12 \pm 0.03$ was found to be representative of most agricultural crops for a variety of view angles (Van de Griend and Wigneron, 2004). This estimate was later refined to 0.08 by Wigneron et al. (2007) after introduction of the view angle dependence of the vegetation thickness in Eq. (3). Similar values (0.12–0.15) have been estimated over grasslands (Saleh et al., 2006b, 2007). In these studies the effect of the litter layer (that is common in grasslands as opposed to crop fields) was also investigated for the first time. These results have suggested that the attenuation effects due to the water content in this layer is higher than in the standing vegetation, leading to the higher values of 0.15 for parameter b . The use of Eq. (3) allows b to be considered as polarisation and incidence angle independent, and therefore values are tabulated depending only on the canopy type.

The variation of the optical depth with view angle is modulated through two 'vegetation structure' parameters tt_h and tt_v which characterize the isotropy of the structure of the standing vegetation; a value of tt_h or $tt_v > 1$ or < 1 will correspond, respectively, to an increase or decrease of τ with the view angle at each polarisation. These are generally set to '1' in the case of isotropic canopies like that of native grasses (Saleh et al., 2007; Wigneron et al., 2007), while values as high as '8' for tt_v have been estimated for vertically dominated crops such as wheat and corn, with tt_h generally closer to unity (Wigneron et al., 2007).

The scattering of the soil microwave signal within the vegetation layer is parameterized with the scattering albedo ω in Eq. (1). Values of ω have been found to be significantly larger than zero only for corn fields and grasslands at V-pol ($\omega_v = 0.05$), and negligible for all the other crop types and at H-pol (Wigneron et al., 2004, 2007). As the dependence of ω on the view angle has not been clearly demonstrated to date in the literature, the value of ω in L-MEB is tabulated only as a function of the vegetation type (i.e., dependence on view angle is neglected).

Among the soil and vegetation parameters that appear in L-MEB, the roughness parameter H_R is one of two which have the largest impact on the soil moisture retrieval accuracy (the other one being the vegetation parameter b). The dependence of this parameter on the surface roughness characteristics (standard deviation of heights SD, autocorrelation length LC, etc.) is nevertheless not well known. Two studies (Mo et al., 1982; Wigneron et al., 2001) found that the best geophysical parameter to model H_R was the roughness slope parameter ($m = SD/LC$), but many studies also observed a significant dependence of parameter H_R on soil moisture (Wigneron et al., 2001; Escorihuela et al., 2007; Saleh et al., 2007). The dependence of H_R on soil moisture has been explained by an effect called "dielectric roughness", believed to be related to a variation of the dielectric properties within the soil which can be caused by non-uniformities in the soil moisture. To date the relationship between H_R and soil moisture has not been well understood, particularly in the case of crops.

Given that, apart for corn fields, the values of H_R over crops with relatively smooth soils were found to be low ($H_R \sim 0.1$ – 0.2) (Jackson et al., 1999; Wigneron et al., 2007), a constant value (i.e., not dependent on soil moisture) of 0.2 was used in this study. However, for grasslands the relationship $H_R = 1.3 - 1.13 * \theta$ proposed by (Saleh et al., 2007) was used in the case of tall grasses with the presence of litter layer (i.e., to compensate for the effect of the layer on the soil emissivity), while a constant value of 0.5 was set for the other cases as estimated by Wigneron et al. (2004) and Saleh et al. (2007).

Estimates of N_{RV} and N_{RH} for Eq. (2), generally considered zero at L-band, have been recently updated through long time series observations over bare soils from the Surface Monitoring Of the Soil Reservoir Experiment (SMOSREX; De Rosnay et al., 2006), with $N_{RV} = -1$ or 0 and $N_{RH} = 0$ or 1 respectively (Escorihuela et al., 2007). Uncertainties on the calibrated values of these two parameters are relatively low (their variability is relatively low over a large range of roughness conditions).

The land cover information for each of the NAFE'05 high resolution sites (see Table 1) was used to extract the most adequate set of parameters to be used in this study for each site from the L-MEB default database. The resulting parameter sets are shown in Table 2. The eight sites fall into three main SMOS surface types: crop (wheat type), grassland with litter and grassland without litter. For all the

Table 2
L-MEB default parameters and high resolution evaluation of the L-MEB soil moisture retrieval

SMOS surface type	High resolution site	Default parameters									Soil moisture retrieval [%v/v]		
		H_R	Q_R	N_{RH}	N_{RV}	tt_h	tt_v	ω_H	ω_V	b	RMSE	r^2	Bias
Grassland without litter (Saleh et al., 2007)	Roscommon	0.5	0	0	0	1	1	0	0.05	0.15	1.6	0.98	-1.3
Grassland with litter (Saleh et al., 2007)	Stanley	1.3–1.13* θ	0	1	0	1	1	0	0.05	0.12	1.3	0.99	0.6
	Dales										3.7	0.85	1.7
	Midlothian										7.4	0.68	2.8
Crop – wheat (Wigneron et al., 2007)	Merriwa P.	0.2	0	0	-1	1	8	0	0	0.08	21.4	0.94	-19.5
	Cullingral										19.4	0.87	-19.2
	Illogan										9.9	0.96	0.4
	Pembroke										32.5	0.95	-30.8

θ is the volumetric soil moisture. Parameters are: roughness (H_R); polarisation mixing (Q_R); roughness exponent (N_{RP}), vegetation structure (tt_p) and scattering albedo (ω_p , all at V and H pol), and vegetation parameter (b).

crop sites, the most suitable parameters were found to be those estimated over crops with mainly vertically oriented plant structure like wheat. In the NAFE'05 study area the predominant crop is wheat followed by barley which has a very similar plant structure. Given that no specific parameters are available in literature for oats, also present at Illogan, this site was assigned the same wheat-type crop parameters. While oats still have a predominantly vertical structure, this is less defined than in wheat and barley. Stanley and Dales were characterized by grazing lands covered by very tall grass, hence the presence of litter on the ground. Roscommon was a very short grass site with exposed, un-littered bare soil between the grass clumps. Midlothian was split between a nearly bare fallow field and a lush, short lucerne field. In the absence of specific literature parameters for the radiative transfer properties of lucerne, it was assumed that the anisotropic structure of lucerne was similar to that of grass clumps. Therefore the site was treated as grassland.

4. High resolution soil moisture retrieval

The accuracy of the L-MEB soil moisture retrieval was tested using the high resolution aircraft observations (62.5 m footprint) over the high resolution soil moisture monitoring sites listed in Table 1. At these sites all the factors known to affect the microwave emission were well monitored, and the spatial variability of soil moisture within the aircraft footprint is known in great detail (6.25 m and 12.5 m spacing). Direct comparison of the L-MEB retrieval with ground measured soil moisture therefore allows detailed evaluation of the effectiveness of the model physics and parameterization with minimum uncertainty on the ancillary data used and on the soil moisture heterogeneity within the pixel.

In order to compare the L-MEB soil moisture retrieval with the ground measurements, PLMR footprints covering each high resolution site were extracted for the nominally 62.5 m resolution data. Approximately 5–8 independent, bi-polarised TB observations of the same area at a variety of incidence angles were available for each high resolution site. A value of ground measured soil moisture was calculated for each observation by averaging all the ground measurements falling within the footprint (Fig. 2). The number of ground measurements per footprint varies due to local topographic conditions affecting the effective footprint size but was generally in the range 50–100 points per footprint.

Fig. 3 shows the observed mean V-pol and H-pol TB together with the mean and standard deviation of the ground measured soil moisture plotted daily at all eight high resolution sites for the four sampling dates available at each individual site. For better visualization, the TB data shown in this plot have been referenced to the same incidence angle (38°) using the ratios between the grand means of TB observations at each incidence angle for each day. As previously discussed, heavy rainfall fell over the entire study area prior to the commencement of the sampling operations, with further rain until November 10th; this is reflected in the very wet conditions observed at all sites on the first two sampling dates, particularly at the sites characterized by clay soils (Pembroke and Stanley). After November 10th and until November 23rd, a gradual drying down was observed. On November 23rd another rainfall event produced moderately wet conditions which were recorded at the two sites monitored after that date (Stanley and Illogan). The whiskers in Fig. 3 indicate the standard deviation of ground measured soil moisture within the high resolution footprint (averaged over the 5–8 footprints falling within each high resolution site and fully ground monitored at high resolution). The soil moisture standard deviation was on average 5.6 %v/v. Maximum spatial variability was recorded at Midlothian (10.0 %v/v) due to the strong contrast between the land cover in the two halves of the high resolution site (fallow field and a lush lucerne crop). High spatial variability was also recorded at Stanley (9.4 %v/v) and Dales (8.8 %v/v) due to the steep topography. Minimum soil moisture heterogeneity was recorded at the Roscommon 'control' site (3.1 %v/v).

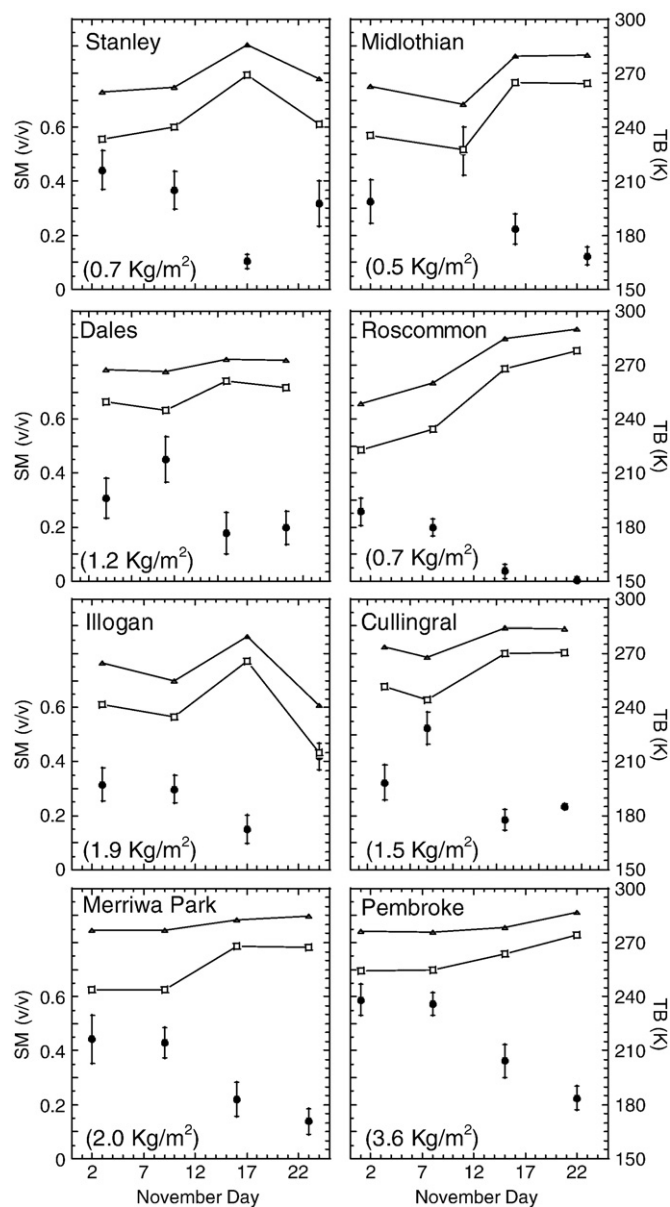


Fig. 3. High resolution brightness temperatures ("TB", lines) and ground measured soil moisture ("SM", solid symbols) plotted daily at the eight high resolution sites. Triangles are V polarised and squares are H polarised brightness temperatures. The temporal mean of the vegetation wet biomass recorded throughout the campaign at each site is indicated in brackets as a reference of the canopy density.

The radiometer data show significant sensitivity to the top 5 cm soil moisture, with higher values of TB for dry soil and lower values on wet soil. The range of TB is slightly higher at H-pol than at V-pol. This effect might have been partially smoothed here by the angle 'correction' applied to the TB data. The H-pol TB show a range of approximately 40 K for a variation in soil moisture around 25 %v/v over low vegetated grasslands (e.g., Roscommon). This range is almost halved to approximately 25 K at sites with crops of higher vegetation biomass (Pembroke, Merriwa Park); as expected, the presence of a mature crop above the ground reduces the sensitivity of TB to soil moisture, although the soil microwave signal is still detectable above the canopy and can be used to retrieve soil moisture.

4.1. Soil moisture retrieval with L-MEB default parameters

The L-MEB soil moisture retrieval was first evaluated using the L-MEB default values for the surface type dependent parameters. Soil moisture

was retrieved at all high resolution sites using a two channel retrieval (H-pol and V-pol) on each TB observation and the resulting soil moisture was compared with the mean ground observed soil moisture within the TB footprint. The value of soil temperatures at 2.5 cm and 15 cm from the nearest permanent monitoring station at the time of TB acquisition were used by the direct emission model to calculate the effective temperature. The value of the VWC estimated daily from the biomass samples collected at the high resolution site was used to characterise the temporally varying contribution of the vegetation to the emission. The temperature of the vegetation canopy was assumed to be in equilibrium with the soil temperature at 2.5 cm; this is a common assumption in passive microwave soil moisture retrieval studies due to the lack of adequate canopy temperature measurements (e.g., Njoku and Entekhabi, 1996; Van de Griend et al., 2003). Analysis of the above canopy infrared measurements recorded at some of the monitoring stations showed that at the time when the high resolution acquisitions considered here were undertaken (9–11AM), the difference between the two temperatures can be significant, more in the case of crops (13 K mean difference) than that of grasses (6 K). The consequences of this uncertainty on the soil moisture retrieval are discussed later in this section.

Fig. 4a shows the scatter plot between L-MEB soil moisture retrieval using the L-MEB default parameters and the ground measured soil moisture. Grassland sites show the best results, with errors generally smaller than the standard deviation of ground measured soil moisture within the footprint. This indicates a good correspondence between ground average soil moisture and sensor-averaged response and a correct parameterization of the model. Over crops the model shows a tendency to underestimate soil moisture, particularly in wet conditions. Error statistics are summarized for each site in Table 2. The Root Mean Square Error (RMSE) between observed and estimated soil moisture was better than the proposed SMOS accuracy (4.0 %v/v) for most grassland sites, while for the crop sites errors up to 32.5 %v/v were obtained. The retrieval error shows a notable correlation with the VWC (compare with Table 1, 5th column), being higher for Pembroke and Merriwa Park, two mature crops, and smaller for the short grasslands at Roscommon and Stanley. This suggests that such large errors could be due to the low default values of parameter *b* tabulated for crops and leading to underestimation of the vegetation opacity. The parameterization of the roughness parameter H_R as a function of soil moisture well reproduced the soil

moisture dynamics for grassland sites, although in the case of Roscommon a successful retrieval was achieved using a constant H_R value (0.5). This is a result of the relatively limited soil moisture range exhibited at the site (below approximately 20 %v/v, Fig. 3) due to the sandy soil texture. It is to be noted that the soil moisture retrieval at the Midlothian site was less accurate than at the other grassland sites. Midlothian was a site with unique land cover conditions in the study area, including a mix of lucerne, for which no parameters were available in literature, and fallow, characterized by significant dead biomass at the surface. This resulted in a strong soil moisture gradient within the high resolution area. It is likely that the combination of these three factors (Incorrect parameterisation, effect of the dead biomass layer and strong soil moisture gradient) determined the error obtained. Given the accurate retrievals at the other grassland site, the Midlothian site was not considered further in the analysis.

The results presented suggest that the set of L-MEB default surface type parameters are directly applicable to Australian conditions in the case of the native grasses present in the NAFE'05 study area. For the wheat-type crops considered in this study, using the default parameters leads to large soil moisture retrieval errors. There are a number of factors that could be the cause of such errors, such as the effect of heterogeneity of the vegetation cover (which was observed to be higher at the crop sites) or error in the estimates of ancillary parameters such as effective temperature, canopy temperature, soil texture and the VWC. A sensitivity analysis of the L-MEB model soil moisture outputs to the value of the input parameters and ancillary data error was performed in order to understand which of these factors could lead to the large errors observed. To this end, starting from a reference scenario with fixed values for all parameters, the values of the input vegetation specific and ancillary parameters were changed within expected ranges individually, while keeping all the other parameters fixed to the reference values. At each step the retrieved soil moisture was then compared to that of the reference scenario to estimate the error in soil moisture retrieval induced by changes in the value of the vegetation specific parameter or errors in the input ancillary data. The process was repeated for 4 scenarios; the mature crop at Pembroke and the short grassland site at Roscommon (see Table 1) for both the wettest and driest conditions (see Fig. 3). This is shown in Fig. 5 and discussed hereby.

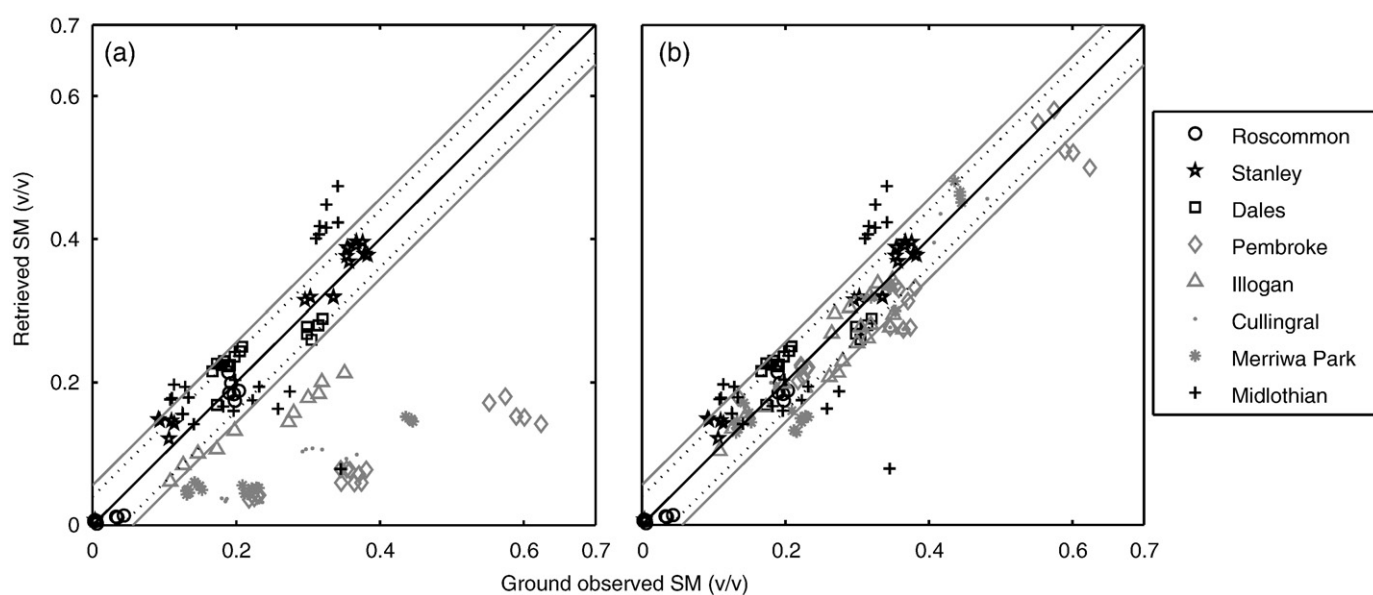


Fig. 4. Evaluation of L-MEB soil moisture (“SM”) retrieval with high resolution aircraft data using (a) L-MEB default parameters and (b) calibrated parameters. Gray symbols are sites classified as crops, black symbols are sites classified as grassland. Black dashed lines indicated the SMOS target accuracy (4 %v/v). Gray lines indicate the typical standard deviation of the ground monitored soil moisture at sub-footprint scale.

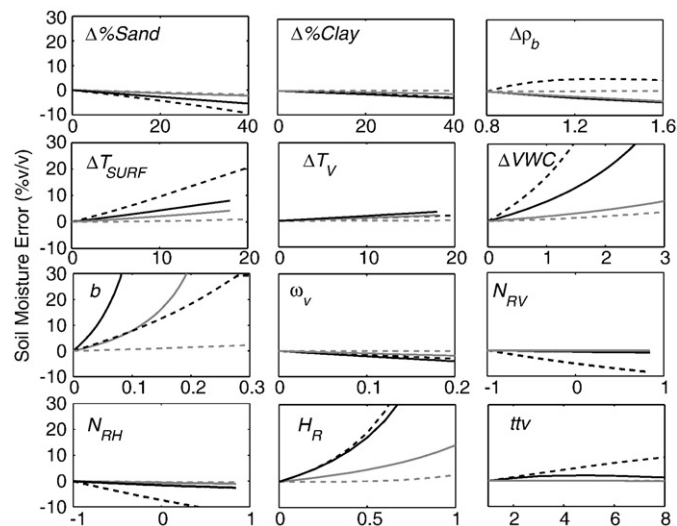


Fig. 5. Analysis of the L-MEB microwave emission model sensitivity to errors in the ancillary data used (top two rows) and changes in the input radiative transfer parameters (bottom two rows) with respect to the reference scenarios of a crop site ($VWC=2.4 \text{ kg/m}^2$, solid lines) and a grassland site ($VWC=0.7 \text{ kg/m}^2$, dashed lines) on wet (black line) and dry (gray line) conditions. ρ_b =soil bulk density [g/cm^3]; T_{SURF} =soil temperature at 2.5 cm [K], T_V =vegetation canopy temperature [K], VWC =vegetation water content [kg/m^2]. All parameters are fixed to the L-MEB default values when not changed.

The top 2.5 cm and 15 cm soil temperatures were estimated using data from monitoring stations which were not always immediately adjacent to the high resolution sites, but rather as much as 1 km distant. This could lead to error in the estimation of the soil effective temperature in the direct emission model. The maximum spatial difference in soil temperature between monitoring stations recorded on sampling days was 6.5 K. It was assumed that this is the maximum error in soil temperature estimation at the high resolution sites and through the sensitivity analysis it was estimated that the associated soil moisture error should not be greater than approximately 5 %v/v. The same analysis revealed that the soil moisture error associated with the assumption that the canopy temperature is in equilibrium with the top 2.5 cm soil temperature at the time of the day when high resolution observations were acquired (9–11AM) should not be greater than approximately 3 %v/v, as this is the maximum soil moisture error observed in Fig. 5 for errors in canopy temperature up to 20 K. For soil textural properties, the values of % sand and % clay were derived from the analysis of 30 cm deep soil samples collected at or nearby the high resolution sites. As there might be a difference between the soil textural properties used and those of the top 5 cm layer which contributes to the soil microwave emission at L-band, a sensitivity study was undertaken showing that large errors in soil textural property estimations can lead to significant errors in retrieved soil moisture only for extreme errors in soil texture (approximately 10 %v/v error for a 40% sand and clay estimate error), which are considered unlikely here.

The VWC sampling technique used (daily 50 cm \times 50 cm biomass samples at 2 fixed locations in the high resolution site) could lead to an error in VWC estimation due to both the small sample size (bound to be heterogeneous in the case of crops, for example) and the spatial variation of the VWC across the area. Analysis of this error using the 16 samples taken on several occasions at each site showed the daily value of the VWC used for crops could be underestimated by approximately 0.12 kg/m^2 for most crops (Cullingral, Illogan and Merriwa Park) and as much as 1 kg/m^2 for Pembroke. The impact of these biases on the soil moisture retrieval was investigated by adding them to the daily VWC recorded at each sites and repeating the retrieval. Results indicated that increasing the VWC improved the RMSE of soil moisture retrieval at Pembroke by 4.1 %v/v, while at the other crop sites the

improvement was only 0.4 %v/v. It is evident that the problem of VWC sampling only marginally accounts for the large errors at the crop sites, although the spatial variation of the VWC across the high resolution sites might explain the scatter observed in daily errors at the same area (Fig. 4a).

Although the errors associated with ancillary data estimation discussed above are in some cases significant and certainly affect the accuracy of the soil moisture retrieval presented here, it is evident that they cannot explain the large errors observed at the crop sites (approximately 20–30 %v/v). This suggests that the errors could be due to the inadequate values of the default parameters when applied to the heterogeneous aircraft footprints. Amongst these, parameters b and H_R are the best candidates, having the highest impact on the L-MEB soil moisture output (Fig. 5).

4.2. Calibration option 1: b and H_R

A site specific calibration of the parameters b and H_R was performed for the crop sites (Pembroke, Merriwa Park, Illogan and Cullingral). Initially, both parameters were jointly calibrated at each site. To this end, all V-pol and H-pol high resolution observations of each site were used together with the ground soil moisture and ancillary data to retrieve both parameters on each sampling day. The temporal average for each parameter was then computed and used to evaluate the soil moisture retrieval on all sampling days, using the same two-channel retrieval described earlier. As already noted, both parameters are considered as view angle independent, as the angular dependence is treated in L-MEB through Eqs. (2) and (3). This implies that one single value of each parameter can be retrieved by using the 5 to 8 TB observations available over each site on each day.

Given that H-pol TB is more sensitive to soil moisture while V-pol responds more to the canopy signal, the simultaneous retrieval of b and H_R is expected to allow decoupling of the soil surface (H_R) from the vegetation (b) component of the observed TB. The value of the calibrated parameters and the respective soil moisture retrieval RMSE are shown in Table 3 ('calibration 1'). The calibration of b and H_R significantly improved the retrieval for most sites. For the site with the highest VWC (Pembroke), the retrieval accuracy was improved from 32.5 %v/v to 8.9 %v/v. The calibrated values of b and H_R were significantly higher than the default ones indicating that the default parameters (i) underestimate the effect of the vegetation layer in masking the soil signal and (ii) underestimate the scattering of the soil signal at the surface. At the Cullingral site very high values of b were obtained. It should be noted that the TB observations available at this site were mostly within a narrow range of incidence angles close to nadir (see Table 3, column 2). At these angles the polarisation difference is reduced and so too is the ability of the algorithm to decouple the vegetation and soil signal. For the remaining sites, the retrieved values for b were in the range 0.2–0.5 while for H_R was in the range 0.2–0.6. These values allowed retrieval of soil moisture with accuracy better than 8.9 %v/v.

4.3. Calibration option 2: H_R alone

The coupled b and H_R calibration presented in the previous section determined a sensible improvement of the L-MEB soil moisture default retrieval over crops. Nevertheless, the accuracy achieved is still far from the 4.0 %v/v accuracy target of SMOS. A second approach was to assume that the default value of parameter b proposed for crops (0.08) is correct and thus calibrate only H_R . This was justified by three reasons: (i) the value 0.08 for wheat-type crops resulted from an extensive review of estimates of b at L-band for various crop types, and therefore it is expected to be quite accurate (Wigneron et al., 2007); (ii) parameter b is expected to be less variable than parameter H_R across the similar wheat-type crops present in the study area and (iii) parameter H_R and its link to geophysical variables (soil type,

Table 3

Site specific calibration of parameters b and H_R and resulting soil moisture RMSE for the NAFE'05 crop sites

High resolution site	Range of incidence angles	Parameter set	b	H_R	Soil moisture RMSE [%v/v]
Merriwa P.	5°–42°	L-MEB default	0.08	0.2	21.4
		Calibration 1	0.26	0.46	6.4
		Calibration 2	0.08	1.03	5.1
		Calibration 3	0.08	$H_R = 1.5 - 1.6 * \theta$	4.8
Cullingrall	6°–23°	L-MEB default	0.08	0.2	19.4
		Calibration 1	1.15	0.46	18.2
		Calibration 2	0.08	1.29	14.5
		Calibration 3	0.08	$H_R = 1.6 - 1.0 * \theta$	3.0
Illogan	3°–44°	L-MEB default	0.08	0.2	9.9
		Calibration 1	0.48	0.19	7.2
		Calibration 2	0.08	0.49	3.5
		Calibration 3	0.08	$H_R = 0.7 - 0.9 * \theta$	2.9
Pembroke	16°–39°	L-MEB default	0.08	0.2	32.5
		Calibration 1	0.19	0.57	8.9
		Calibration 2	0.08	1.12	8.0
		Calibration 3	0.08	$H_R = 1.6 - 1.2 * \theta$	4.0

All retrieved values averaged across four dates. θ indicates soil moisture. 'Calibration 1' = calibration of both b and H_R ; 'calibration 2' = calibration of only H_R , b fixed to default; 'calibration 3' = calibration of linear regression of H_R vs soil moisture, b fixed to default.

surface roughness and soil moisture) have not yet been well understood.

For all sites a significant improvement in soil moisture accuracy was achieved when calibrating H_R alone (see Table 3, 'calibration 2') with respect to the calibration of both b and H_R , soil moisture retrieval improved for all sites with an improvement of at least 1.0 %v/v and up to 3.7 %v/v in some cases. Calibrated values of H_R were in the range 0.5–1.3, being much higher than both the default values (0.1–0.2) and those obtained in 'calibration 1' (0.2–0.5). Although this is partly a result of having constrained parameter b to a fixed (low) value, which might therefore partially absorb the underestimation of the vegetation opacity, these results suggest that the default value of parameter H_R for crops is too low for the crop types considered in this study.

4.4. Calibration option 3: H_R as a function of soil moisture

In calibrations 1 and 2 the parameters b and H_R were considered stable in time, i.e., one average value was calculated from the calibration on individual days to evaluate the soil moisture retrieval. An examination of the retrieved values of both parameters across the 4 sampling dates showed that while parameter b was fairly constant in time (as expected given that it relates to the vegetation structure) the values of parameter H_R exhibited a notable variation in time, and this was fairly consistent with the soil moisture conditions. In particular, higher values of H_R were derived for dry soils. This is consistent with several previous studies over crops and grasslands (Wigneron et al., 2001; Escorihuela et al., 2007; Saleh et al., 2007). The dependence of H_R on soil moisture could be explained by an effect of volume scattering: as the soil dries out, emission originates from deeper layers within the soil. Possibly, the spatial fluctuations of the dielectric constant within the soil volume are strong during drying out, producing an important "dielectric" roughness effect. Therefore, H_R could be considered as an effective parameter that accounts for (i) "geometric roughness" effects, in relation with spatial variations in the soil surface height, and (ii) "dielectric roughness" effects in relation with the variation of the dielectric constant at the soil surface and within the soil which can be caused by non-uniformities in the soil characteristics.

In line with these studies, a simple linear regression was used to model the relationship between H_R and soil moisture and the effect of this assumption on the soil moisture retrieval accuracy investigated. The site specific regression coefficients are shown in Table 3 ('calibration 3') together with the associated soil moisture retrieval

RMSE. An improvement in soil moisture retrieval accuracy was achieved at all sites after calibration of the soil moisture dependence of H_R . In particular, RMSE was reduced by 11.5 %v/v at Cullingrall and by 4.0 %v/v at Pembroke. For Merriwa Park and Illogan the improvement was not significant, indicating that at these sites a fairly accurate soil moisture retrieval is achieved without a soil moisture dependent parameterization of H_R . After calibration of H_R , soil moisture could be retrieved with an accuracy better than 4.8 %v/v at all the sites analyzed except Midlothian (RMSE = 7.4 %v/v). Scatter plots of the retrieved versus ground measured soil moisture after calibration are shown in Fig. 4b.

The coefficients of the regression of H_R as a function of soil moisture obtained were quite uniform across the four crop sites. In particular, the slope of the relationship for the different crops was in the range 0.9–1.6, which is close to the 1.3 already observed for grasslands by Saleh et al. (2007). The resulting value of H_R decreased on average from 1.3 on very dry soils (5.0 %v/v) to 0.8 on very wet soils (50.0 %v/v). At Illogan, low values of both the slope and intercept of the regression were retrieved, resulting in lower and more stable values of H_R with respect to soil moisture. A hypothesis was made to relate the slope and intercept of the regression to soil geophysical parameters such as soil texture, standard deviation of surface height (SD) and surface roughness autocorrelation length (LC) available for each site (see Table 1). However, the relative narrow range of surface roughness conditions and soil types available across the four sites makes it difficult to generalize our observations.

5. Summary and conclusions

In this study the L-MEB model, which is core to the future SMOS level 2 processor, was evaluated using L-band passive microwave aircraft observations at 62.5 m resolution over a variety of vegetation covers, soil types and topography under Australian conditions. Unprecedented spatial detail in soil moisture monitoring allowed rigorous validation of the model. This study is unique in that the L-MEB model, developed and tested using tower-mounted radiometers, has never before been applied to aircraft observations over such a large area, and never before on Australian conditions.

Soil moisture was retrieved with an accuracy better than 4.8 %v/v on all the surface types considered when using site specific calibration of roughness parameter H_R . However, the L-MEB default parameter set of vegetation and surface specific parameters was found to be suitable only for grasslands (maximum error 3.7 %v/v), with crops errors as high as 32.5 %v/v. It was suggested that the L-MEB default values of H_R are too low for the vertically dominated crops (wheat and barley) analysed in this study. Moreover, a linear parameterization of H_R as a function of soil moisture was necessary to achieve soil moisture accuracy better than 5.0 %v/v for crop sites. This is consistent with previous results obtained using tower mounted radiometer both over grasslands and crops in Europe (Wigneron et al., 2001; Saleh et al., 2007), and is also in line with observations over the NAFE'05 study area by an independent study using the EMIRAD radiometer (Saleh, person. comm.). The next step will be that of understanding whether the impact of roughness on the soil moisture retrieval is sensitive to the spatial resolution of observation, and therefore whether it will constitute a problem at the scale of satellite footprints as well. This problem will be addressed in the near future using the NAFE'05 airborne measurements over mixed pixels made at larger scale (about 1 km).

Acknowledgment

The authors would like to thank the NAFE'05 participants. The National Airborne Field Experiment 2005 has been made possible through recent infrastructure (LE0453434) and research (DP0557543) funding from the Australian Research Council, and the collaboration

of a large number of scientists from throughout Australia, United States and Europe. The authors also wish to thank Cristina Martinez for providing the laser mastersizer soil particle analysis data.

References

- Campbell, J. R. (2003). Limitations in the laser particle sizing the soils. In R. I.C. (Ed.), *Advances In Regolith* (pp. 38–42). : CRC LEME.
- Della Vecchia, A., Ferrazzoli, P., Wigneron, J. P., & Grant, J. P. A. G. J. P. (2007). Modeling forest emissivity at L-band and a comparison with multitemporal measurements. *IEEE Geoscience and Remote Sensing Letters*, 4(4), 508–512.
- De Rosnay, P., Calvet, J. -C., Kerr, Y., Wigneron, J. -P., Lemaitre, F., Escorihuela, M. J., et al. (2006). SMOSREX: A long term field campaign experiment for soil moisture and land surface processes remote sensing. *Remote Sensing of Environment*, 102(3–4), 377–389.
- Dobson, M. C., Ulaby, F. T., Hallikainen, M. T., & El-Rayes, M. A. (1985). Microwave dielectric behavior of wet soil—part II: Dielectric mixing models. *IEEE Transactions on Geoscience and Remote Sensing*, GE-23(1), 35–46.
- Escorihuela, M. J., Kerr, Y. H., de Rosnay, P., Wigneron, J. P., Calvet, J. C., & Lemaitre, F. (2007). A simple model of the bare soil microwave emission at L-band. *IEEE Transactions on Geoscience and Remote Sensing*, 45(7), 1978–1987.
- Grant, J. P., Wigneron, J. P., Van de Griend, A. A., Kruszewski, A., Sobjaerg, S. S., & Skou, N. (2007). A field experiment on microwave forest radiometry: L-band signal behaviour for varying conditions of surface wetness. *Remote Sensing of Environment*, 109(1), 10–19.
- Jackson, T. J. (1993). Measuring surface soil moisture using passive microwave remote sensing. *Hydrological Processes*, 7, 139–152.
- Jackson, T. J., & Le Vine, D. E. (1996). Mapping surface soil moisture using an aircraft-based passive microwave instrument: Algorithm and example. *Journal of Hydrology*, 184(1–2), 85–99.
- Jackson, T. J., Le Vine, D. M., Hsu, A. Y., Oldak, A., Starks, P. J., Swift, C. T., et al. (1999). Soil moisture mapping at regional scales using microwave radiometry: The Southern Great Plains Hydrology Experiment. *IEEE Transactions on Geoscience and Remote Sensing*, 37(5), 2136–2151.
- Jackson, T. J., & Schmugge, T. J. (1991). Vegetation effects on the microwave emission of soils. *Remote Sensing of Environment*, 36(3), 203–212.
- Jackson, T. J., Schmugge, T. J., & O'Neill, P. (1984). Passive microwave remote sensing of soil moisture from an aircraft platform. *Remote Sensing of Environment*, 14(1–3), 135–151.
- Jackson, T. J., Schmugge, T. J., & Wang, J. R. (1982). Passive microwave sensing of soil-moisture under vegetation canopies. *Water Resources Research*, 18(4), 1137–1142.
- Kerr, Y. H., Waldteufel, P., Wigneron, J. P., Martinuzzi, J. M., Font, J., & Berger, M. (2001). Soil moisture retrieval from space: The Soil Moisture and Ocean Salinity (SMOS) mission. *IEEE Transactions on Geoscience and Remote Sensing*, 39(8), 1729–1735.
- Matzler, C. (1998). Microwave permittivity of dry sand. *IEEE Transactions on Geoscience and Remote Sensing*, 36(1), 317–319.
- Merlin, O., Walker, J., Panciera, R., Young, R., Kalma, J., & Kim, E. (2007). *Soil Moisture Measurement in Heterogeneous Terrain. International Congress on Modelling and Simulation (MODSIM)*. Christchurch, New Zealand.
- Mo, T., Choudhury, B. J., Schmugge, T. J., Wang, J. R., & Jackson, T. J. (1982). A model for the microwave emission of vegetation-covered fields. *Journal of Geophysical Research*, 87(11), 229–237.
- Njoku, E. G., & Entekhabi, D. (1996). Passive microwave remote sensing of soil moisture. *Journal of Hydrology*, 184(1–2), 101–129.
- Njoku, E. G., Wilson, W. J., Yueh, S. H., Dinardo, S. J., Li, F. K., Jackson, T. J., et al. (2002). Observations of soil moisture using a passive and active low-frequency microwave airborne sensor during SGP99. *IEEE Transactions on Geoscience and Remote Sensing*, 40(12), 2659–2673.
- Panciera, R., Walker, J. P., Kalma, J. D., Kim, E. J., Hacker, J., Merlin, O., et al. (2008). The NAFE'05/CoSMOS data set: Towards SMOS soil moisture retrieval, downscaling and assimilation. *IEEE Transactions on Geoscience and Remote Sensing*, 46(3), 736–745.
- Rüdiger, C., Hancock, G., Hemakumara, H. M., Jacobs, B., Kalma, J. D., Martinez, C., et al. (2007). Goulburn River experimental catchment data set. *Water Resources Research*, 43, (W10403).
- Saleh, K., Wigneron, J. -P., de Rosnay, P., Calvet, J. -C., Escorihuela, M. J., Kerr, Y., et al. (2006a). Impact of rain interception by vegetation and mulch on the L-band emission of natural grass. *Remote Sensing of Environment*, 101(1), 127–139.
- Saleh, K., Wigneron, J. -P., de Rosnay, P., Calvet, J. -C., & Kerr, Y. (2006b). Semi-empirical regressions at L-band applied to surface soil moisture retrievals over grass. *Remote Sensing of Environment*, 101(3), 415–426.
- Saleh, K., Wigneron, J. P., Waldteufel, P., de Rosnay, P., Schwank, M., Calvet, J. C., et al. (2007). Estimates of surface soil moisture under grass covers using L-band radiometry. *Remote Sensing of Environment*, 109(1), 42–53.
- Talone, M., Camps, A., Moneris, A., Vall-llossera, M., Ferrazzoli, P., & Piles, M. (2007). Surface topography and mixed-pixel effects on the simulated L-band brightness temperatures. *IEEE Transactions on Geoscience and Remote Sensing*, 45(7), 1996–2003.
- Van de Griend, A. A., & Wigneron, J. P. (2004). The b-factor as a function of frequency and canopy type at H-polarization. *IEEE Transactions on Geoscience and Remote Sensing*, 42(4), 786–794.
- Van de Griend, A. A., Wigneron, J. P., & Waldteufel, P. (2003). Consequences of surface heterogeneity for parameter retrieval from 1.4-GHz multiangle SMOS observations. *IEEE Transactions on Geoscience and Remote Sensing*, 41(4), 803.
- Wang, J. R. (1983). Passive microwave sensing of soil moisture content: The effects of soil bulk density and surface roughness. *Remote Sensing of Environment*, 13(4), 329–344.
- Wang, J. R., & Choudhury, B. J. (1981). Remote sensing of soil moisture content over bare field at 1.4 GHz frequency. *Journal of Geophysical Research*, 86, 5277–5282.
- Wigneron, J. P., Calvet, J. C., Pellarin, T., Van de Griend, A. A., Berger, M., & Ferrazzoli, P. (2003). Retrieving near-surface soil moisture from microwave radiometric observations: Current status and future plans. *Remote Sensing of Environment*, 85(4), 489–506.
- Wigneron, J. P., Chanzy, A., Calvet, J. C., & Bruguier, N. (1995). A simple algorithm to retrieve soil moisture and vegetation biomass using passive microwave measurements over crop fields. *Remote Sensing of Environment*, 51(3), 331.
- Wigneron, J. -P., Kerr, Y., Saleh, K., Richaume, P., de Rosnay, P., Escorihuela, M. -J., et al. (2008). Parameterisation and calibration of L-MEB in the Level-2 SMOS algorithm. *10th Specialist Meeting on Microwave Radiometry and Remote Sensing of the Environment, Abstract and invited oral communication*. Florence, Italy.
- Wigneron, J. P., Kerr, Y., Waldteufel, P., Saleh, K., Escorihuela, M. J., Richaume, P., et al. (2007). L-band Microwave Emission of the Biosphere (L-MEB) Model: Description and calibration against experimental data sets over crop fields. *Remote Sensing of Environment*, 107(4), 639–655.
- Wigneron, J. P., Laguerre, L., & Kerr, Y. H. (2001). A simple parameterization of the L-band microwave emission from rough agricultural soils. *IEEE Transactions on Geoscience and Remote Sensing*, 39(8), 1697–1707.
- Wigneron, J. P., Parde, M., Waldteufel, P., Chanzy, A., Kerr, Y., Schmidl, S., et al. (2004). Characterizing the dependence of vegetation model parameters on crop structure, incidence angle, and polarization at L-band. *IEEE Transactions on Geoscience and Remote Sensing Letters*, 42(2), 416–425.